JOURNAL OF MATERIALS SCIENCE 38 (2003) 2293–2297

Thermal conductivity of a kaolinite refractory: effect of a plant-derived organic binder

A. A. OGACHO, B. O. ADUDA, F. W. NYONGESA
Department of Physics, University of Nairobi, P.O. Box 30197, Nairobi-Kenya
E-mail: boaduda@uonbi.ac.ke

The effect of *corchorus olitorius* derived binder on the effective thermal conductivity of a kaolinite-based refractory was investigated. Strong dependence of (effective) thermal conductivity of fired samples on the binder concentration, temperature and porosity was noted. Comparison of experimental data with Effective Medium Approximation (EMA) and Geometric Mean Model (GMM) theories showed that predictions from EMA agreed better with the experimental data than those from GMM. This was attributed to the EMA model being more rigorous and contained more microstructural information than the simpler GMM.

1. Introduction

Thermal conductivity is a property that controls the thermo-mechanical behavior of refractory linings, and hence their design and optimization. It further determines the heating and cooling schedules of these linings. As such, the control and knowledge of thermal conductivity of refractory materials used in various conditions is a necessity.

In the ceramics industry, use of organic binders during processing of components is not uncommon [1–5]. The organic binders, besides improving mechanical [5] and/or thermal properties [4] have the additional advantage of minimizing production losses associated with breakage and cracking of the green ware.

In a recent study [5] it was noted that kaolinite refractories plasticized using a binder (syrup) extracted from an edible vegetable (*corchorous olitorius*), had higher fracture strength compared to those samples fabricated using only plain tap water as the plasticizer. This feature was attributed to the observed change in fracture paths from intergranular to transgranular with increasing binder concentrations. In this study, we report the variation of (effective) thermal conductivity of a similar kind of kaolinite refractory fabricated using the binder derived from *corchorous olitorius*, and also compare the experimental data with theoretical values calculated using EMA and GMM theories. This type of refractory and others based on clays are used as thermal insulators for metal cooking stoves.

2. Experimental procedures

2.1. Materials

In the present study Kaolin clay (supplied by Athi River Mining Company, Athi River Kenya) and fresh leaves of *corchorus olitorius* vegetable bought from a local market were used. The binder was extracted by gently heating at 100°C, a known mass ($\approx 500 \pm 5$ g) of the fresh leaves in a known volume (500 ± 5 cm^3) of tap water for half an hour. A longer heating time than this resulted in the undesired cooking of the leaves. The resulting thick dark-green slimy syrup was cooled to room temperature, sieved to remove any residues of leaf fibres, and then subsequently stored in a domestic fridge. This process was repeated until enough of the syrup was obtained. The separately extracted batches of the syrup were finally mixed together in a large bucket and thoroughly stirred to ensure uniformity of the initially undiluted concentration. Different concentrations (measured in terms of viscosity η) of the binder were eventually prepared by diluting a fixed volume (V_o) of the undiluted syrup of viscosity η_o with varying volumes V, of tap water. Finally the concentrations were normalized with respect to the viscosity of the undiluted binder (η_o).

Different sets of kaolin pastes were made by mixing a given mass of kaolin clay with 33 wt% of the binder (of different concentrations). This way, the kaolin was plasticized with binders of different concentrations. The mixture was kneaded to obtain uniform dough, which was left overnight to age. Semi-cylindrical samples (15.0 ± 0.1 cm long and 5.0 ± 0.1 cm in diameter) were then fabricated for thermal conductivity measurements. These specimens were left to dry at room temperature for seven (7) days, oven-dried further at 120 ± 5°C for eight hours and then stored in moisture free chambers. All samples were fired at the rate of 5 K min^{-1} to a peak temperature of 1150°C, soaked at this temperature for 30 ± 1 min and thereafter allowed to cool to room temperature overnight.

2.2. Thermal conductivity measurement

The transient hot wire method was used to measure the thermal conductivities of samples under test. In this method, the heater wire (nichrome wire—standard wire gauge SWG 36) and thermocouple (nichrome/constantan both of SWG 36) hot wires' junction were sandwiched between two

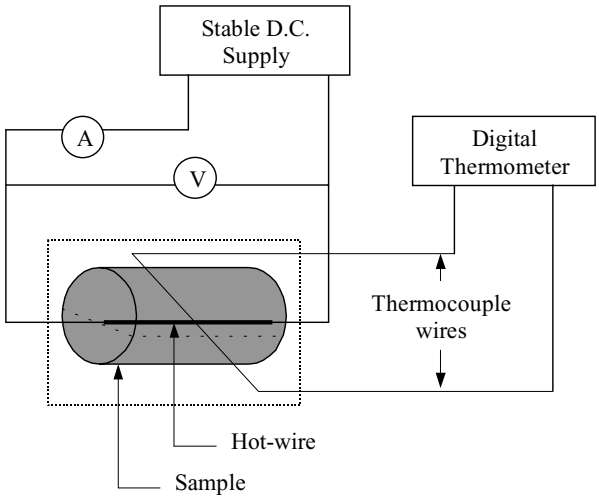

Figure 1 Experimental set up for thermal conductivity measurement by transient hot-wire technique.

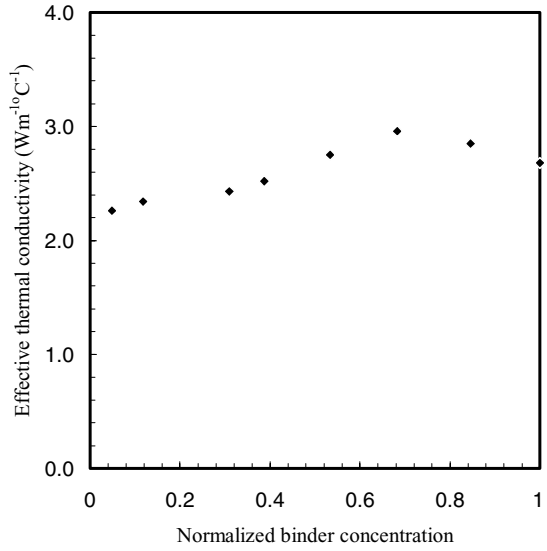

Figure 2 Variation of effective thermal conductivity with binder concentration at room temperature.

semi-cylindrical specimens as shown in Fig. 1. To ensure good thermal contact between the heater wire and the test sample, the heater wire was squeezed into the small central grooves running lengthwise on each half of the test pieces.

To obtain data for the thermal conductivity K determination, a steady current I, per unit length was passed through the probe for three (3) minutes then switched off. The input power (Q) per unit length of the hot wire was determined from the voltage (V) across the heater wire and current (A) through the wire. The heater wire surface temperature $T(a, t)$ was registered by a digital thermometer (*Fluke 38501*), where 'a' is the radius of the hot wire. Time t versus the hot wire surface temperature $T(a, t)$ was recorded at 10 s intervals during heating up and cooling down.

For measurements above the room temperature, the sample, with the measuring unit coupled to it (part enclosed by the dotted rectangle) were placed inside a furnace which was then heated to and held at the desired temperature for sufficient time to allow samples' body temperature to stabilize within $\pm 0.1^{\circ}$C/min, and the conductivity data taken as previously described. A plot of $T(a, t)$ versus natural logarithm of time t ($\ln t$) gave a straight line whose gradient was determined by the "least squares" method. The absolute values of the slopes of graphs obtained from data collected during heating, and cool down were averaged and used to calculate the effective thermal conductivity at the temperature of interest from the relation [6]

$$T(a, t) = \frac{Q}{4\pi K} \ln t \tag{1}$$

In order to ascertain the reliability of system, the same system was used to measure the thermal conductivity of Pyrex glass at 20°C, where a value of 1.03 ± 0.06 W/m/°C was obtained compared to the reported value of 1.1 W/m/°C [7].

3. Results and discussions

Fig. 2 shows the variation the measured effective thermal conductivity ($K_{\text{eff.}}$) with binder concentration at room temperature ($23.5 \pm 0.5^{\circ}$C).

It is noted that thermal conductivity increases gradually from 2.26 $\text{Wm}^{-1}\,^{\circ}\text{C}^{-1}$ (for samples plasticized with plain water) to a maximum of 2.96 $\text{Wm}^{-1}\,^{\circ}\text{C}^{-1}$ (at normalized binder concentration of 0.683) followed by a slight decrease at higher binder concentrations. This represents an increase of about 20%. This trend is the same even at higher temperatures as depicted in Fig. 3). The increase in thermal conductivity could be attributed to reduction in porosity, which has been observed to fall (from an initially high value to a minimum followed by a small increase) with increasing binder concentration [5, 8]. The reduced porosity occasioned by plasticization with the vegetable syrup may be as result of the increased liquid phase during the sintering process associated with the enhanced amount of fluxes from the syrup [5]. The subsequent drop in thermal conductivity can be explained thus: During the sintering process, the organic matter contained in the vegetable syrup (binder) volatilizes and leaves behind some residual pores. The amount of residual porosity left behind should increase with the syrup (binder

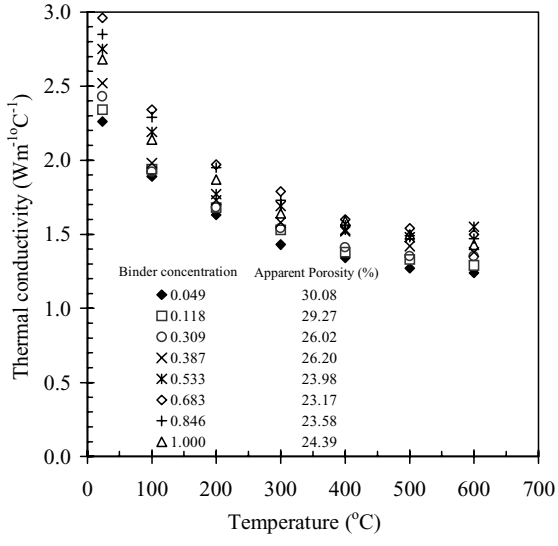

Figure 3 The variation of thermal conductivity with temperature, binder concentration and porosity.

concentration) since more concentrated syrup contains more volatilizable matter. Higher amount of residual pores therefore should be responsible for the slight fall in the $K_{\text{eff.}}$ observed beyond the (optimal) binder concentration (0.683). Note that the fall in the thermal conductivity occurs only when the increase in porosity due to volatilization process exceeds the decrease in porosity due to enhanced sintering. It is known that at room temperature the thermal conductivity of a solid phase is higher than that of a gaseous phase. Thus the amount of porosity present in the sample controls the thermal behaviour as observed in Fig. 2 above.

Fig. 3 illustrates the variation of (effective) thermal conductivity with temperature and porosity. It is seen that $K_{\text{eff;}}$ monotonously decreases nonlinearly with increasing temperature, but with ever-smaller rates at higher temperatures. This pattern indicates that the dominant mode of heat transfer was solid (lattice) conduction, though radiative heat transfer was gradually becoming important at elevated temperatures. In fact the rather small but noticeable upturn in thermal conductivity around 600°C is owed to enhanced contribution by the radiative heat transfer. The contribution to the effective thermal conductivity by the fluid, herein assumed to be air is effectively limited by the micropores present in the specimens. Also distinguishable from Fig. 3 is the fact that a fixed temperature, the thermal conductivity decreases with increasing porosity.

3.1. Comparison of theoretical models with experimental data

The experimental results were compared with theoretical results of the Effective Medium Approximation (EMA) and the weighted Geometric Mean Model (GMM) as given by Equations 2 and 3 respectively [9–13]. In the present study we used Bruggeman's symmetrical effective medium approximation (EMA) theory that assumes 3-3 connectivity schemes where it is visualized that the medium is built up from self-connecting spherical phases. The thermal conductivity of such a medium is then calculated from Bruggeman's equation [10],

$$f\frac{k_1 - k_{\text{eff.}}}{k_{\text{eff.}} + l_1(k_1 - k_{\text{eff.}})} + (1-f)\frac{k_2 - k_{\text{eff.}}}{k_{\text{eff.}} + l_2(k_2 - k_{\text{eff.}})} = 0 \qquad (2)$$

where k_1, k_2 and $k_{\text{eff.}}$ are the thermal conductivities of phase 1, phase 2 and the composite respectively, f is the volume fraction of phase 1, and the depolarization factors of the two phases being l_1 and l_2. We further assume spherical grains and set both depolarization factors—l_1 and l_2 to 1/3. Substituting both l_1 and l_2 with 1/3 in Equation 2 above and solving for $k_{\text{eff.}}$ yields Equation 3 [11, 12]

$$K_{\text{eff.}} = \frac{1}{4}\{(3\phi_1 - 1)K_1 + (3\phi_2 - 1)K_2 + \langle[(3\phi_1 - 1)K_1 + (3\phi_2 - 1)K_2]^2 + 8K_1K_2\rangle^{\frac{1}{2}}\} \qquad (3)$$

The geometric mean equation employed in this study is

$$K_{\text{eff.}} = K_1^{\phi_1}K_2^{\phi_2}K_3^{\phi_3}, \ldots, K_n^{\phi_n} \qquad (4)$$

where $\phi_1, \phi_2, \phi_3, \ldots, \phi_n$ are the volume fractions of the constituent phases, while $K_1, K_2, K_3, \ldots, K_n$ are the conductivity of these phases respectively.

To facilitate the calculation of the thermal conductivity of the solid component at zero porosity, the chemical analysis data of Aduda *et al*. [5] together with the thermal conductivity data of the oxides from Kaye and Labby [7], and Botteril *et al*. [14] were used as described elsewhere [15]. The solid phase (zero porosity) was thus estimated as ~4.30 $\text{Wm}^{-1}\ \text{K}^{-1}$ at 20°C, assuming the solid component (kaolinite) to be made of crystalline $SiO_{2\|}$ and crystalline Al_2O_3 only. This assumption was justified on the basis that the other oxides that constitute the kaolin used in this study were present only in very small quantities that did not significantly affect the thermal conductivity of the solid phase at zero porosity.

Since the thermal conductivity of the gaseous phase (assumed to be air) also increases with temperature, we used the following expression to determine the gas conductivity at elevated temperatures (above room temperature)

$$K_{\text{air}} = 0.0237 + 6.4 \times 10^{-5}\,T \qquad (5)$$

where T is temperature [16].

To take account of the contribution to thermal conductivity by radiation, a radiative term calculated using Equation 6 [17] was added to the theoretical results obtained from Equations 3 and 4.

$$K_{\text{R}} = \frac{16n_{\text{R}}^2\sigma_{\text{R}}T^3}{3e} \qquad (6)$$

where n_{R} (≈1.56) is the refractive index, σ_{R} is Stefan Boltzmann constant, T is the mean temperature (absolute) and e is the extinction coefficient (e/ρ = mass extinction coefficient ≈ 1.2 ± 0.2 m^2/g for kaolin, ρ is the density) [18, 19] of the matrix. The results shown in Fig. 4, indicate that the contribution of the radiative heat transfer component increased by about 30 times, within the temperature range covered (23.5–577.0°C) but its net input remained small throughout, such that even at 577.0°C, as it was still 600 times less than the solid conduction term, albeit increasing.

Figs 5 and 6 show the comparisons between the experimental thermal conductivity data at two different porosities ($P = 23.17\%$ and 30.08%) with the theoretical results based on the EMA and the GMM theories respectively.

From both Figs 5 and 6, it is observed that the EMA model gives predictions that are closer to the experimental values as compared to the GMM model. This apparent good agreement of the EMA model with the experimental data could be attributed to the number of characteristic parameters that have been considered in

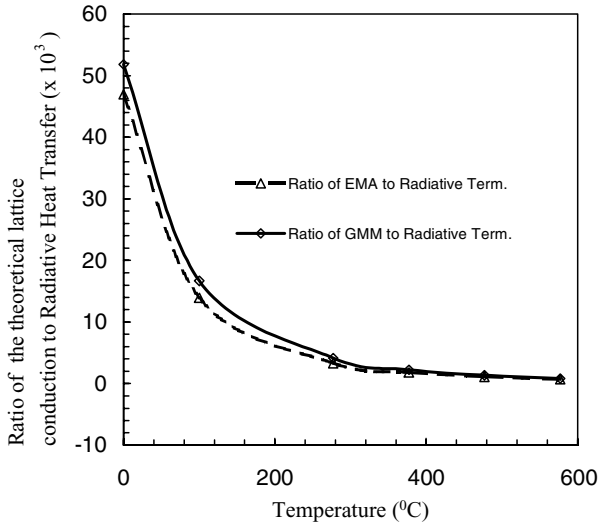

Figure 4 The ratio of solid (lattice) conduction component (theoretical results) to radiative (photon) thermal conduction.

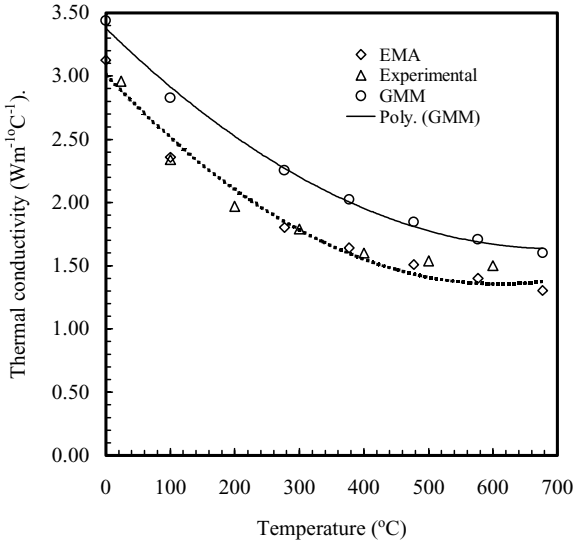

Figure 5 Comparison of the theoretical results (GMM and EMA) with the experimental results (of sample plasticized with binder of optimal concentration (0.683), and porosity $P = 0.27$).

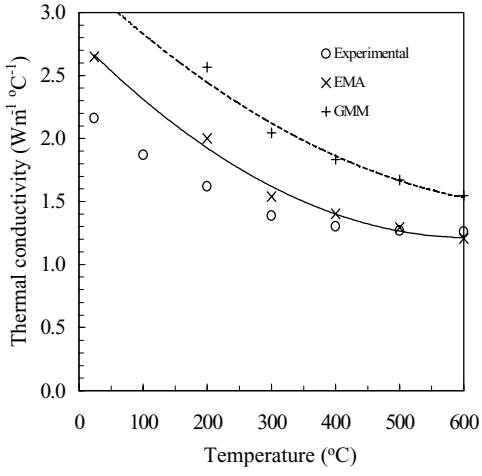

Figure 6 Comparison of theoretical results (GMM and EMA) with experimental data ($P = .30$).

describing the microstructure of the material under test. Notably, the GMM considers phase volume fractions and porosity, which are barely adequate for full characterization of a complex composite, like the one studied here, whereas the EMA takes into account a number of these parameters, including constituent phases' volume fractions and connectivity, pore shape, pore distributions and their orientation [10]. It should be pointed out that in Figs 5 and 6 it would be expected that all the calculated values should lie on the respective curves. The slight departure from this expectation is attributed to the estimation procedure used in calculated the solid phase thermal conductivity at various temperatures.

4. Conclusions

The effective thermal conductivity of fired samples showed strong dependence on the binder concentration, temperature and porosity. Up to a level, higher binder concentrations were shown to give higher values of measured thermal conductivity. Effective medium approximations theory agreed better with the experiment compared to Geometric Mean Model. The results of effective thermal conductivity indicated that the dominant mode of heat transfer was solid conduction. Calculated values of the radiative heat transfer component increased at higher temperatures (above 100°C) but its overall contribution remained significantly low compared to the solid conduction component. These results show that this vegetable-derived binder can be used to cheaply make reasonably strong thermal clay or kaolin thermal insulators that become more effective even as temperature rises.

Acknowledgements

The authors wish to thank the International Program in Physical Sciences (IPPS) of Uppsala University Sweden for partial funding of the project, and the University of Nairobi for providing scholarship to AAO, and research facilities.

References

1. J. A. BREWER, R. H. MOORE and J. S. REED, *Amer. Ceram. Soc. Bull.* **68**(2) (1981) 212.
2. H. TANAKA, S. FUKAI, N. UCHIDA, K. UEMATSU, A. SAKAMOTO and Y. NAGAO, *J. Amer. Ceram. Soc.* **77**(12) (1994) 3077.
3. S. BAKLOUTI, T. CHARTIER and J. F. BAUMARD, *ibid.* **80**(8) (1997) 1992.
4. S. PARK and J. G. HARTLEY, *J. Appl. Phys.* **86**(9) (1999) 5263.
5. B. O. ADUDA, F.W. NYONGESA F. W. and G. OBADO, *J. Mater. Sci. Lett.* **18** (1999) 1653.
6. P. G.KNIBBE, *Int. J. Heat Mass Transfer* **29**(3) (1986) 463.
7. G. W. C. KAYE and T. H. LABBY, "Tables of Physical and Chemical Constants and Some Mathematical Functions" 5th ed. (Longmans, London, 1986).
8. A. A. OGACHO, MSc. Thesis, University of Nairobi, Kenya, 2002.
9. B. HAKANSSON and R. G. ROSS, *J. Appl. Phys.* **68** (1990) 3285.
10. A. BJORNEKLETT, L. HAUKELAND, J. WIGREN and H. KRISTIANSEN, *J. Mater. Sci.* **29** (1994) 4043.

11. R. LANDAUER, *J. Appl. Phys.* **23**(7) (1952) 779.
12. A. D. BRAILSFORD and K. G. MAJOR, *Brit. J. Appl. Phys.* **15** (1964) 313.
13. F. PASCAL and F. W. JONES, *Geophys. J. Int.* **118** (1994) 623.
14. J. S. M. BOTTERIL, A. G. SALWAY and Y. TEOMAN, *Int. J. Heat Mass Transfer* **32**(3) (1989) 595.
15. B. O. ADUDA, *J. Mater. Sci.* **31** (1996) 6441.
16. A. K. SHROTRIYA, *Indian J. Pure and Appl. Phys.* **29** (1991) 339.
17. P. G. COLLISHAW and J. R. G. EVANS, *J. Mater. Sci.* **29** (1994) 2261.
18. X. LU, P. WANG, C. ARDUINI-SHUSTER, J. KUHN, D. BUTTNER, O. NILSSON and O. HEINEMANN, *J. Non-Cryst. Sol.* **145** (1992) 207.
19. J. D. TIMOTHY and S. A. WILLIAMS, www.cira.colostateie.edu/GeoSci/Bacimo2000/

Received 28 October 2002
and accepted 26 February 2003